Bioorganic & Medicinal Chemistry Letters
journal homepage: www.elsevier.com

Discovery of a D-Pro-Lys peptidomimetic inhibitor of MMP9: addressing the gelatinase selectivity beyond S1' subsite

Elena Lenci,[a,*] Alessandro Contini,[b] Andrea Trabocchi[a,c,*]

[a] *Department of Chemistry "Ugo Schiff", University of Florence, Via della Lastruccia 13, 50019 Sesto Fiorentino, Florence, Italy*
[b] *Department of Pharmaceutical Sciences, University of Milan, Via Venezian 21, I-20133 Milan, Italy*
[c] *Interdepartmental Center for Preclinical Development of Molecular Imaging (CISPIM), University of Florence, Viale Morgagni 85, 50134 Florence, Italy*

* Corresponding author. Phone, +39 055 4573507; fax, +39 055 4574913; E-mail, andrea.trabocchi@unifi.it, elena.lenci@unifi.it.

ARTICLE INFO

Article history:
Received
Received in revised form
Accepted
Available online

Keywords:
Peptidomimetics
Amino acids
Enzyme inhibition
Angiogenesis
Matrix metalloproteinase
Drug discovery

ABSTRACT

Despite a high degree of structural similarity, it is known that MMP2 and MMP9 have distinct roles in the angiogenic switch and in cell migration, as they activate diverse signaling pathways. Indeed, inhibition of MMP2 and MMP9 can show beneficial or detrimental effects depending on the stage of tumor progression. Thus, the selective inhibition of gelatinases is of relevance for a successful drug lead, which has to be achieved despite the high structural similarity of the two gelatinases. Herein, the synthesis and evaluation of D-proline-derived hydroxamic acids containing amino appendages at C-4 as gelatinase inhibitors are reported. Inhibition assays enabled the identification of a >200-fold selective MMP9 inhibitor when Lys was considered as a C-4 substituent, thus addressing gelatinase selectivity beyond the S1′ subsite, which is a major driver for selectivity. Molecular docking studies revealed the basic moiety of Lys as detrimental for inhibition of MMP2 as compared to MMP9.

Although the investigation of matrix metalloproteinase (MMP) inhibitors have begun over three decades ago, these enzymes are receiving a renewed interest for the development of therapies targeting angiogenesis and metastasis hallmarks, as it is now clear that initial MMP inhibitor clinical trials were held prematurely.[1] The failure of MMP inhibitors as drug candidates in clinical trials has been mainly attributed to (a) inhibition of other metalloenzymes, (b) low oral availability due to poor pharmacokinetics and *in vivo* instability, (c) lack of specificity within the MMP family.[2] This latter issue is particularly significant when the aim is the development of compounds targeting the gelatinases subfamily. In fact, although both gelatinase A (MMP2) and B (MMP9) are secreted, zinc-dependent endopeptidases involved in the regulation of cell growth, migration, invasion, inflammation and angiogenesis, their subsequent effects on cancer cell survival and migration is substantially different.[3] High levels of either MMP2 and MMP9 are found in many human malignancies, including those of breast, brain, pancreas, colon-rectum, lung, bladder, skin, prostate,[4] and are often associated with tumor aggressiveness and poor prognosis.[5] However, different roles have been observed for these two enzymes in the angiogenic switch,[6] in platelet function,[7] and in cell migration,[8] as they activate diverse signaling pathways. For example, it has been shown that in A549 lung cancer cells, MMP2 interacts with integrin $\alpha_v\beta_3$ inducing the PI3/AKT signaling pathway, that activates hypoxia-induced transcription factor-1α (HIF-1α) and expression of the vascular endothelial growth factor VEGF (Figure 1a).[9]

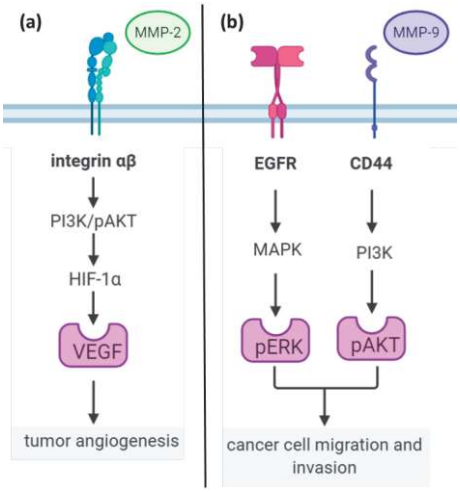

Figure 1. Schematic representations of the signaling pathways leading to tumor angiogenesis and cancer cell migration and invasion induced by (**a**) MMP2 and (**b**) MMP9.

Differently, in several tumor epithelial cells of kidney, breast and fibrosarcoma, MMP9 interacts with CD44 and tyrosine kinase epidermal growth factor receptor (EGFR), inducing the

downstream PI3K/AKT cell signaling cascade that favors cancer cell migration and invasion (Figure 1b).[10] Also, it has been demonstrated how MMP2 and MMP9 inhibition can show beneficial or detrimental effects depending on the stage of tumor progression.[11] Thus, the selective inhibition of gelatinases is of relevance for a successful clinical trial, which has to be achieved despite the high structural similarity of the two gelatinases.[12] Previous studies showed how the substitution at the nitrogen atom of proline-derived compounds with chemical functions linking 1 to 3 rings within the *N*-arylsulfonyl moiety was successful in identifying highly potent and selective MMP2 inhibitors addressing the deep and hydrophobic S1' subsite.[13] In order to advance towards this direction, we reasoned to explore the molecular recognition determinants beyond S1' subsite by bifunctional molecules, to improve the inhibition selectivity between the two gelatinases (Figure 2).[5] Thus, a series of novel D-proline peptidomimetic derivatives possessing the same arylsulfonyl hydrophobic group at the nitrogen atom and amine-containing groups at position 4 of the pyrrolidine ring were synthesized and assayed. The incorporation of amino groups at C-4 was envisioned to provide hydrogen bonding interactions and to furnish a suitable functional group for subsequent bioconjugation strategies.

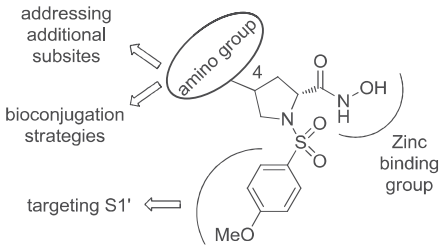

Figure 2. General structure of 4-substituted D-proline derivatives developed in this work.

The key intermediate (2*R*,4*R*)-methyl 1-((4-methoxyphenyl)sulfonyl)-4-amminopyrrolidine-2-carboxylate (**4**) was obtained in good yield starting from *trans*-4-hydroxy-D-proline **1**, by following a previously reported strategy (Scheme 1).[14] *Trans*-4-hydroxy-D-proline was left reacting with thionyl chloride in methanol and subsequent sulfonamide formation gave the functionalized proline compound **2** in 60% yield. The *p*-methoxyphenyl group was installed as a reference moiety to address the S1' pocket of the two gelatinase enzymes, without inducing a significant selectivity. Then, the Mitsunobu reaction on **2** with diphenylphosphoryl azide (DPPA) produced azide **3** with inverted configuration at the C-4 stereocenter in 85% yield, that was then subjected to catalytic hydrogenation using 10% Pd/C to give amine **4** in 92% yield.

Compound **4** proved to be a good starting point to introduce amides at position 4 of the pyrrolidine scaffold (Scheme 2). In particular, in order to address potential acidic residues in the S2 pocket, different amino acids containing amino group functionalities in diverse positions were taken into account, specifically *N*-Boc-L-norleucine **5**, *N*-Boc-γ-aminobutyric acid (GABA) **6**, *N*α-Boc-*N*ε-Cbz-L-ornithine **7** and *N*α-Boc-*N*ε-Cbz-L-lysine **8**.

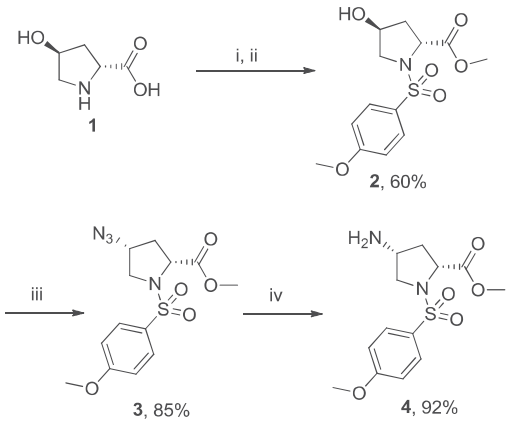

Scheme 1. Synthesis of the key intermediate **4**. Reagents and conditions: (i) $SOCl_2$, MeOH, r.t., 16 h; (ii) 4-methoxybenzenesulfonyl chloride, Et_3N, DMAP, dry CH_2Cl_2, N_2, 0 °C to r.t., 16 h; (iii) PPh_3, DIAD, DPPA, dry THF, -15 °C to 60 °C, 40 minutes; (iv) H_2, Pd/C 10%, HCl (cat.), r.t., 16 h.

The corresponding coupling products **9-10** and **15-16** were obtained in good to high yields by a standard procedure with 1-hydroxybenzotriazole (HOBt) and *N*-(3-dimethylaminopropyl)-*N'*-ethylcarbodiimide (EDC), although **5** and **6** proved to be slightly less reactive. The methyl ester of compounds **9** and **10** was then directly converted into the hydroxamic acid by aminolysis with NH_2OK/NH_2OH in MeOH, and Boc protecting group was removed under acidic conditions to give final compounds **13-14** in quantitative yields (Scheme 2, left). Differently, the methyl ester of compounds was transformed into the hydroxamic acid by a two-step procedure consisting of the hydrolysis with LiOH and subsequent coupling reaction with *N*-benzylhydroxylamine hydrochloride to give intermediates **17-18** in 75% and 51% yields, respectively. Successively, Cbz and Bn protecting groups were removed by hydrogenation under Pd/C catalysis to obtain compounds **19** and **20**, and Boc protecting groups were removed under acidic conditions to give final compounds **21** and **22** in good to excellent yields (Scheme 2, right). Finally, compound **4** was left reacting with pivaloyl chloride in order to introduce a bulky apolar group as reference control. The corresponding intermediate **23** was then treated with NH_2OK/NH_2OH in MeOH, thus giving compound **24** in 35% yield, in agreement with previous data about low performance of this transformation (Scheme 2, middle).[13]

The inhibition potency of the series of hydroxamic acid derivatives (against MMP2 and MMP9 was evaluated through a fluorometric assay using 96-well plates and the fluorogenic substrate Mca-Lys-Pro-Leu-Gly-Leu-Dpa-Ala-Arg-NH_2, at excitation and emission wavelengths of 320 and 420 nm, respectively. For all the compounds, IC_{50} values were obtained by dose-response measurements using an inhibitor range of concentrations (0.1 nM-100 μM) and enzyme concentration equal to 1 nM. The inhibition activities of the synthesized compounds towards the two gelatinases, as reported in Table 1, were then compared with the reference compound **25**, previously synthesized in our laboratories,[13] possessing the same *p*-methoxylbenzylsulfonyl appendage to address S1', but no chemical moieties at position 4 of the pyrrolidine ring. These results suggested that the amino-containing appendages play a key role in driving the selectivity towards the two gelatinases.

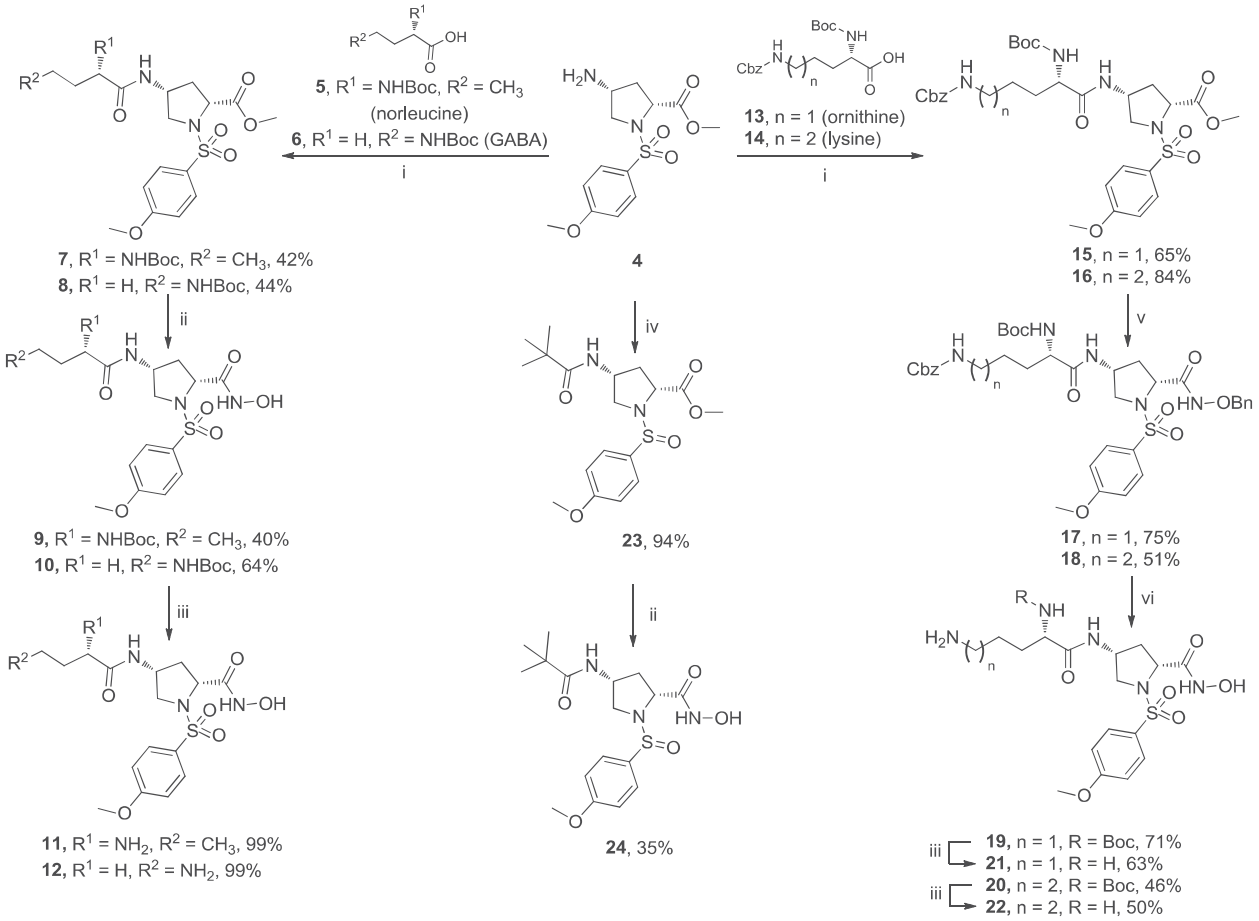

Scheme 2. Synthesis of D-proline derived hydroxamic acids functionalized at position 4**.** Reagents and conditions: (i) HOBT, EDC, TEA, DCM, 0 °C to r.t., 72 h; (ii) NH_2OH, KOH, MeOH, 80 °C, m.w., 1 h; (iii) HCl (4M in dioxane), 0 °C to r.t., 1 h; (iv) pivaloyl chloride, TEA, DCM, 0 °C to r.t., 16 h; (v) NH_2OBn, HOBT, EDC, TEA, DCM, 0 °C to r.t., 72 h; (vi) H_2, Pd/C 10%, HCl (cat.), r.t., 16 h.

In fact, although compounds **11** and **12** (functionalized with norleucine and γ-aminobutyric acid, respectively) displayed poor MMP2/MMP9 selectivity, as for the reference compounds **24** and **25** and even slightly lower inhibition potency, the introduction of ornithine and lysine side chains proved to be successful in achieving selective inhibitors for both the two gelatinases. In fact, compound **21**, possessing a shorter chain, proved to inhibit preferentially MMP2 enzyme, with an IC_{50} value of 15 nM, while compound **22**, with a longer chain, showed a reverse propensity, inhibiting MMP9 enzyme with an IC_{50} value of 5.7 nM and a 220-fold selectivity in favour of this enzyme. A similar inhibition preference was observed for their corresponding Boc-protected derivatives **19-20**, although with lower potency and less significant enzyme selectivity. Similarly, compounds **9** and **10**, characterized by the presence of Boc-protected norleucine and γ-aminobutyric acid, showed a decrease in the inhibition potency towards MMP2 and MMP9, suggesting the free amino group playing a role for the selective interaction with the enzymes. Given the selectivity observed for compounds **21** and **22**, such compounds were selected for further investigations through molecular docking and dynamics studies, in order to identify the molecular determinants responsible for the selectivity switch observed for these two compounds among the two gelatinases.

Compounds **21** and **22** were docked into MMP2 and MMP9 and the top-scored poses were refined by MD simulations, followed by MM-GBSA binding energy calculations. Computed binding energy for the lowest-energy poses are reported in Table 2, while representation of the binding poses are depicted in Figure 3. The binding energy values (ΔG_{bind}) reported in Table 2 are in a very good match with the experimental findings, in particular for the values obtained by the more accurate MM-GBSA calculations. Indeed, a significant difference in ΔG_{bind} was obtained for **22** bound to MMP2 and MMP9, with a $\Delta\Delta G_{bind}$ of 25.3 kcal/mol in favour of the latter enzyme. The values obtained by the docking scoring function (GBVI/WSA dG) also match the experimental ranking. However, the difference between the two enzymes (0.5 kcal/mol) is less evident and well below the mean absolute error of such a scoring method.[15] The same holds for the docking of **21** to MMP2 and MMP9, where the scoring function fails to correctly ranking the two complexes, but only by 0.1 kcal/mol in favour of MMP9. Conversely, MM-GBSA calculations provided again energy values that match well with experiments. Indeed, a higher affinity has been calculated for **21** toward MMP2, which results favoured by 6.9 kcal/mol over MMP9. Compound **22** shows a potency that is >200-fold higher for MMP9 than for MMP2. The inhibitor found in the experimental structure of MMP2 used here as a reference (compound SC-74020)[16] presents the hydroxamic function bound to the Zn atom, the sulfonyl oxygens bound to Ala84 and Val83 backbone NH and the long hydrophobic tail occupying the S1′ pocket. When observing compound **22** bound to MMP2 (Figure 3, A1) the hydroxamic moiety is similarly able to bind the Zn atom. However, the sulfonyl moiety, not involved in any hydrogen-bond with the backbone, points towards the solvent. Moreover, the aryl group occupies the position where the SO_2 group of SC-74020 is found in 1HOV, thus outside the hydrophobic S1' pocket.

Table 1. Binding activity data of D-proline-derived compounds determined using a fluorogenic peptide substrate.

Cmpd	Structure	IC_{50} MMP2, nM	IC_{50} MMP9, nM	MMP9 / MMP2 selectivity	Cmpd	Structure	IC_{50} MMP2, nM	IC_{50} MMP9, nM	MMP9 / MMP2 selectivity
9	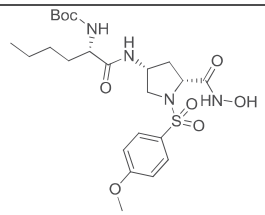	87 ± 9	131 ± 23	1.5	**11**	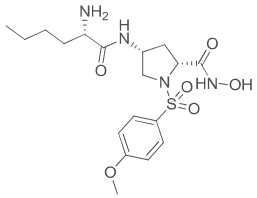	62 ± 22	98 ± 19	1.5
10	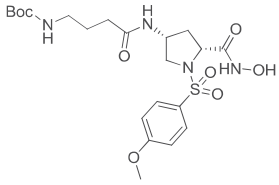	91 ± 16	49 ± 11	0.5	**12**	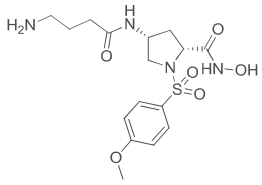	302 ± 92	53 ± 4	0.2
19	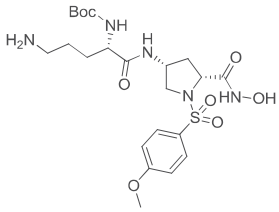	1320 ± 324	3420 ± 1130	2.5	**21**	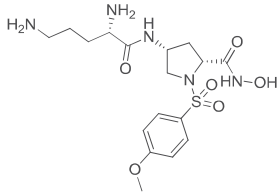	**15 ± 4.5**	**154 ± 73**	**10**
20	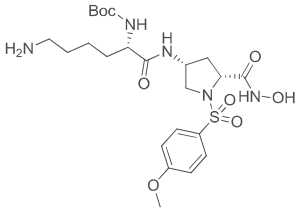	432 ± 103	27 ± 5.4	0.06	**22**	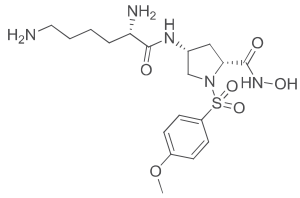	**1260 ± 462**	**5.7 ± 3.7**	**0.005**
24	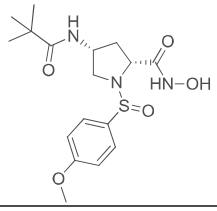	26 ± 7	13 ± 6	0.5	**25**	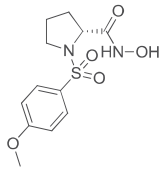	8.9 ± 1.6	22 ± 4	2.5

Table 2. Docking and MM-GBSA binding energies[a] computed for **21** and **22** bound to MMP2 and MMP9 metalloproteases

	MMP2		**MMP9**	
	Docking	MM-GBSA[b]	Docking	MM-GBSA[b]
21	-8.9	-337.9±7.4	-9.0	-331.0 ± 8.6
22	-7.8	-288.2 ± 8.2	-8.3	-313.5 ± 7.0

[a] The binding energy, in kcal/mol, is reported for the most favoured pose resulting from the MM-GBSA analysis. [b]Entropy contribution is neglected for MM-GBSA calculations.

The lysine chain also points towards the solvent, and the terminal ammonium group makes a hydrogen-bond with Glu129. However, this solvent-exposed hydrogen-bond is not probably able to significantly affect the potency of **21**, as suggested by both experimental IC_{50} and theoretical binding energies. Conversely, as shown in Figure 3, B1, the same compound bound to MMP9 shows a binding mode that is much more similar to that of the reverse hydroxamate inhibitor observed experimentally as in the 1GKC PDB file.[17] Indeed, in addition to the interactions with the catalytic Zn, such inhibitor shows hydrogen-bonds with the NH of Leu188 and the carbonyl of Pro421. These interactions are also observed for **22** through the sulfonyl group and both the amido group at C-4 of the proline scaffold and the ammonium group at Cα of the lysine appendage. Moreover, the methoxyphenyl group of **22** occupies the same position in the hydrophobic S1' pocket as observed for the isobutyl group of the reverse hydroxamate inhibitor in 1GKC. Indeed, **22** makes similar hydrophobic contacts with Leu188, His401 and Tyr423. Also in this case, the lysine chain points towards the solvent and, apparently, do not make any particular interaction with the enzyme.

Concerning compound **21**, similar binding modes were obtained for both MMP2 and MMP9 (Figure 3, A2 and B2, respectively), as expected from comparing IC_{50} values and computed binding energies. Moreover, the binding pose of **21** in MMP2 shows analogies with that of the experimental data of the reference ligand SC-74020. Indeed, in addition to the similar geometry of the Zn-binding hydroxamic function, the aryl sulfonyl moieties of the two ligands are also equally oriented into the S1' pocket. Furthermore, **21** shows an additional hydrogen-bond between both the amido NH and the ammonium cation at C-α and Pro140 carbonyl group. Although this hydrogen-bond is not observed for SC-74020, it can be found for different inhibitors of MMP2 and other MMPs. Similar considerations can be done for MMP9, where **21** shows a hydrogen-bonding network similar to that described for the reverse hydroxamate inhibitor in the 1GKC PDB file.[17]

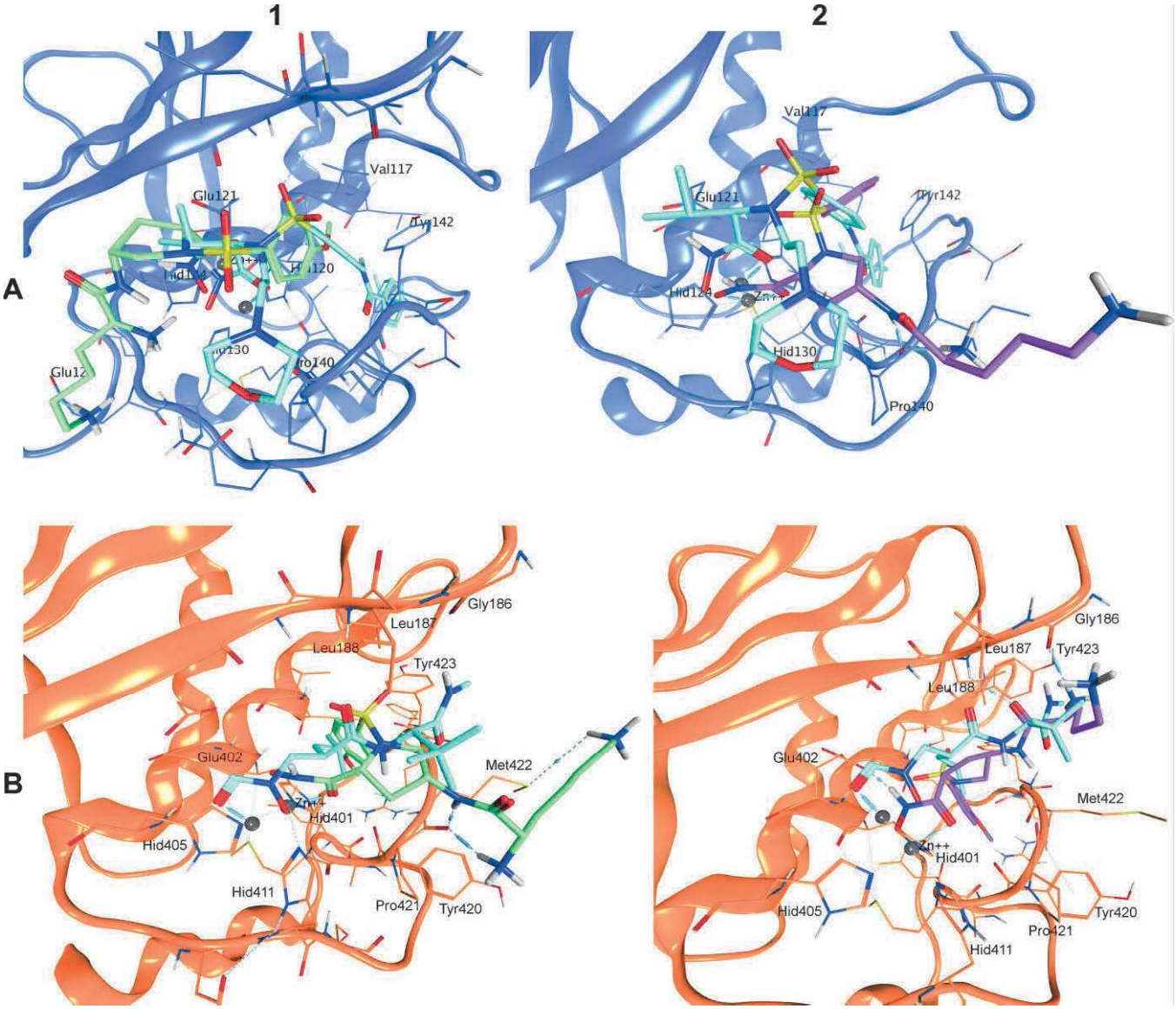

Figure 3. Comparison between the binding poses obtained by docking of **22** and **21** (represented by green and magenta sticks in columns 1 and 2, respectively) to MMP2 and MMP9 (represented as light blue and orange ribbons in rows A and B, respectively) and that of the corresponding experimental ligands (represented as cyan sticks) found in the 1HOV and 1GKC PDB files. Residue numbering is referred to the MMP2 and MMP9 structures as found in the 1HOV and 1GKC PDB files, respectively. The geometries of MMP2 and MMP9 bound to **22** and **21** were obtained by a cluster analysis of the last 10 ns of MD trajectory, followed by geometry minimization of the representative structure of the most populated cluster. The placement of the experimental ligand was done by superposing the 1HOV or 1GKC PDB structures to the afore-mentioned MMP2 and MMP9 complexes, respectively.

Indeed, we observe a hydrogen-bond interaction between the NH of Leu188 and the amido carbonyl of compound **21**. Another hydrogen-bond is observed between Gly186 carbonyl and the ammonium group at the amidic C-α, but the interaction of the same group with the Pro421 carbonyl group, as observed for **22**, appears to be lost. Similarly to other inhibitors, the aryl sulfonyl moiety is well buried in the S1' pocket formed by Leu188, Val398, His401 and Tyr423. Despite the good match between theoretical and experimental results, we were not able to identify a clear reason behind the so different behaviour observed for compounds **21** and **22** in terms of selectivity. In order to hypothesize that the geometry of compound **22** bound to MMP2 might be a docking artifact, we repeated MD simulations and MM-GBSA analysis starting from a complex manually generated by overlying the binding pose of **22** complexed to MMP9, considered as reliable, to MMP2 (Figure S1, Supporting Information). After a restrained geometry minimization to relax eventual steric clashes, the complex was subjected to the same protocol as described above. However, comparable results were obtained in terms of both binding energy (-281.3±7.0 kcal/mol) and geometry (see Table S1 and Figure S2-S5, Supporting Information), except for the lysine chain that was found interacting with the side-chain of Tyr74 instead of Glu129. Based on these results, we can conclude that the MMP2 binding site cannot fit well **22**, specifically due to the longer diamino chain probably forced in interactions with residues outside the binding pocket reducing the anchoring to the Zn and hydrophobic S1' subsites, that are not accessible by **21** and are not favoured when **22** binds to MMP9.

In conclusion, in view of expanding the class of selective gelatinase inhibitors based on D-proline scaffold, we synthesized and evaluated a series of derivatives possessing a basic amino acid at C-4 atom of the pyrrolidine ring. When unprotected lysine and ornithine were considered as C-4 appendages, a selective inhibition towards the two gelatinases was observed, with an inverted trend based on the amino acid present on the molecule. Specifically, the lysine derivative provided >200-fold selectivity towards MMP9, possibly as a result of impaired fit within MMP2

catalytic site. Molecular modeling calculations showed binding energy values in good match with the experimental findings, and binding poses supported that lysine appendage interacts differently within the two enzymes, and for MMP9 guarantees higher activity and potential applications in bioconjugation strategies thanks to the solvent-exposed conformational preference.

Acknowledgments

Financial support from Fondazione Cassa di Risparmio di Pistoia e Pescia (Bando Giovani@Ricerca scientifica 2018, fellowship to EL), Fondazione CR Firenze (cod. 2017.0721), MIUR ("Progetto Dipartimenti di Eccellenza 2018-2022" allocated to Department of Chemistry "Ugo Schiff") and CNR Roadmap Europea ESFRI:CISPIM are acknowledged.

Supplementary data

Supplementary data associated with this article [Experimental procedures and characterization data for all new compounds, copies of ^{1}H and ^{13}C NMR spectra of all new compounds, additional docking and MD results for compounds **21** and **22** and PDB coordinates of the ligand and binding site residues] can be found, in the online version.

References and notes

1. (a) Fields, G. B. *Cells* **2019**, *8*, 984; (b) Cathcart, J.; Pulkoski-Gross, A.; Cao, J. *Genes Dis.* **2015**, *2*, 26-34; (c) Pavlaki, M.; Zucker, S. *Cancer Metastasis Rev.* **2003**, *22*, 177-203; Coussens, L. M.; Fingleton, B.; Matrisian, L. M. *Science* **2002**, *295*, 2387-2392; (d) Nuti, E.; Tuccinardi, T.; Rossello, A. *Curr. Pharm. Des.* **2007**, *13*, 2087-2100; (e) Overall, C. M.; Kleifeld, O. *Nat. Rev. Cancer* **2006**, *6*, 227-239.
2. (a) Sela-Passwell, N.; Rosenblum, G.; Shoham, T.; Sagi, I. *Biochim. Biophys. Acta* **2010**, *1803*, 29–38; (b) Tauro, M.; McGuire, J.; Lynch, C. C. *Cancer Metastasis Rev.* **2014**, *33*, 1043–1057.
3. (a) Vihinen, P.; Ala-aho, R.; Kahari, V. M. *Curr. Cancer Drug Targets* **2005**, *5*, 203-220; (b) Fingleton, B. *Expert Opin. Ther. Tar.* **2003**, *7*, 385-397; (c) Yong, V. W.; Power, C.; Forsyth, P.; Edwards, D. R. *Nat. Rev. Neurosci.* **2001**, *2*, 502-511; (d) George, S. J. *Expert Opin. Inv. Drug* **2000**, *9*, 993-1007.
4. Turpeenniemi-Hujanen, T. *Biochimie*, **2005**, 87, 287-297.
5. Bauvois, B. *BBA Rev. Cancer* **2012**, *1825*, 29-36.
6. Bergers, G.; Brekken, R.; Mcmahon, G.; Vu, T. H.; Itoh, T.; Tamaki, K.; Tanzawa, K.; Thorpe, P.; Itohara, S.; Werb, Z.; Hanahan, D. *Nat. Cell Biol.* **2000**, *2*, 737–744.
7. Fernandez-Patron, C.; Martinez-Cuesta, M. A.; Salas, E.; Sawicki, G.; Wozniak, M.; Radomski, M. W.; Davidge, S. T. *Thromb. Haemostasis* **1999**, *82*, 1730–1735.
8. Giannelli, G.; Falk-Marzillier, J.; Schiraldi, O.; Stetler-Stevenson, W. G.; Quaranta, V. *Science* **1997**, *277*, 225–228.
9. Chetty, C.; Lakka, S. S.; Bhoopathi, P.; Rao, J. S. *Int. J. Cancer* **2010**, *127*, 1081–1095.
10. Dufour, A.; Zucker, S.; Sampson, N. S.; Kuscu, C.; Cao, J. *J. Biol. Chem.* **2010**, *285*, 35944–35956.
11. (a) Vandenbroucke, R. E.; Libert, C. *Nat. Rev. Drug Discov.* **2014**, *13*, 904-927; (b) Higashi, S.; Miyazaki, K. *Biol. Chem.* **2008**, *283*, 10068-10078; (c) Overall, C. M.; Kleifeld, O. *Br. J. Cancer* **2006**, *94*, 941-946.
12. (a) Sluijter, J. P.; de Kleijn, D. P.; Pasterkamp, G. *Cardiovasc. Res.* **2006**, *69*, 595-603; (b) Deryugina, E. I.; Quigley, J. P. *Cancer Metastasis Rev.* **2006**, *25*, 9-34; (c) Haas, T. L. *Can. J. Physiol. Pharmacol.* **2005**, *83*, 1-7.
13. (a) Lenci, E.; Innocenti, R.; Di Francescantonio, T.; Menchi, G.; Bianchini, F.; Contini, A.; Trabocchi, A. *Bioorg. Med. Chem.* **2019**, *27*, 1891-1902; (b) Natchus, M. G.; Bookland, R. G.; De, B.; Almstead, N. G.; Pikul, S.; Janusz, M. J.; Heitmeyer, S. A.; Hookfin, E. B.; Hsieh, L. C.; Dowty, M. E.; Dietsch, C. R.; Patel, V. S.; Garver, S. M.; Gu, F.; Pokross, M. E.; Mieling, G. E.; Baker, T. R.; Foltz, D. J.; Peng, S. X.; Bornes, D. M.; Strojnowski, M. J.; Taiwo, Y.O. *J. Med. Chem.* **2000**, *43*, 4948-4963.
14. (a) Calugi, C.; Trabocchi, A.; Lalli, C.; Guarna, A. *Eur. J. Med. Chem.* **2012**, *56*, 96-107; (b) Bianchini, F.; Calugi, C.; Ruzzolini, J.; Menchi, G.; Calorini, L.; Guarna, A.; Trabocchi, A. *Med. Chem. Commun.* **2015**, *6*, 277-282.
15. Naïm, M.; Bhat, S.; Rankin, K. N.; Dennis, S.; Chowdhury, S. F.; Siddiqi, I.; Drabik, P.; Sulea, T.; Bayly, C. I.; Jakalian, A.; Purisima, E. O. *J. Chem. Inf. Model.* **2007**, *47*, 122-133.
16. Feng, Y.; Likos, J. J.; Zhu, L.; Woodward, H.; Munie, G.; McDonald, J. J.; Stevens, A. M.; Howard, C. P.; De Crescenzo, G. A.; Welsch, D.; Shieh, H.-S.; Stallings, W. C. *BBA Proteins and proteomics* **2002**, *1598*, 10-23.
17. Rowsell, S.; Hawtin, P.; Minshull, C. A.; Jepson, H.; Brockbank, S. M. V.; Barratt, D. G.; Slater, A. M.; McPheat, W. L.; Waterson, D.; Henney, A. D.; Pauptit, R. A. *J. Mol. Biol.* **2002**, *319*, 173-181.